THE JOURNAL OF BIOLOGICAL CHEMISTRY VOL. 289, NO. 20, pp. 13851–13857, May 16, 2014
© 2014 by The American Society for Biochemistry and Molecular Biology, Inc. Published in the U.S.A.

ELIC-α7 Nicotinic Acetylcholine Receptor (α7nAChR) Chimeras Reveal a Prominent Role of the Extracellular-Transmembrane Domain Interface in Allosteric Modulation*

Received for publication, October 3, 2013, and in revised form, March 10, 2014 Published, JBC Papers in Press, April 2, 2014, DOI 10.1074/jbc.M113.524611

Tommy S. Tillman[‡], Edom Seyoum[‡], David D. Mowrey[‡§], Yan Xu[‡¶‖], and Pei Tang[‡§¶1]

From the Departments of [‡]Anesthesiology, [¶]Pharmacology and Chemical Biology, [§]Computational and Systems Biology, and [‖]Structural Biology, University of Pittsburgh School of Medicine, Pittsburgh, Pennsylvania 15260

Background: Allosteric modulators bound to the transmembrane domain (TMD) of the α7 nicotinic acetylcholine receptor (α7nAChR) can potentiate channel function.
Results: ELIC-α7nAChR showed potentiation only when the extracellular-transmembrane domain (ECD-TMD) interface matched that of α7nAChR.
Conclusion: PAM modulation through the TMD requires a more specific ECD-TMD interface than agonist activation.
Significance: The study provides insight into the basis for positive allosteric modulation of α7nAChR.

The native α7 nicotinic acetylcholine receptor (α7nAChR) is a homopentameric ligand-gated ion channel mediating fast synaptic transmission and is of pharmaceutical interest for treatment of numerous disorders. The transmembrane domain (TMD) of α7nAChR has been identified as a target for positive allosteric modulators (PAMs), but it is unclear whether modulation occurs through changes entirely within the TMD or changes involving both the TMD and the extracellular domain (ECD)-TMD interface. In this study, we constructed multiple chimeras using the TMD of human α7nAChR and the ECD of a prokaryotic homolog, ELIC, which is not sensitive to these modulators, and for which a high resolution structure has been solved. Functional ELIC-α7nAChR (EA) chimeras were obtained when their ECD-TMD interfaces were modified to resemble either the ELIC interface (EA_{ELIC}) or α7nAChR interface ($EA_{\alpha7}$). Both $EA_{\alpha7}$ and EA_{ELIC} show similar activation response and desensitization characteristics, but only $EA_{\alpha7}$ retained the unique pharmacology of α7nAChR evoked by PAMs, including potentiation by ivermectin, PNU-120596, and TQS, as well as activation by 4BP-TQS. This study suggests that PAM modulation through the TMD has a more stringent requirement at the ECD-TMD interface than agonist activation.

The α7 nicotinic acetylcholine receptor (α7nAChR)[2] is a homopentameric acetylcholine-gated cation channel mediating fast synaptic transmission in neuronal cells (1) and calcium signaling in nonneuronal cells (2). The diverse biological functions of α7nAChR have made it a promising therapeutic target for numerous medical conditions, including pain (3, 4), inflammation (5), cardiovascular disease (6), and a variety of psychiatric and neurological disorders (7–9). α7nAChR opens the channel gate in the transmembrane domain (TMD) upon agonist binding to the extracellular domain (ECD), but channel function can also be modulated by ligand binding to allosteric sites distinct from the orthosteric agonist binding-sites in the ECD. Positive allosteric modulators (PAMs), especially those specific for α7nAChR, such as PNU-120596 (10) and TQS (11), are particularly of therapeutic potential (8). Based upon mutational analysis, certain PAMs are thought to act at the ECD or ECD-TMD interface (12, 13), whereas others, such as PNU-120596 and TQS, are thought to act through binding to intrasubunit sites near the middle of the α7nAChR TMD (13–17). The molecular mechanisms of allosteric modulation are not understood.

α7nAChR is a member of the pentameric ligand-gated ion channel (pLGIC) superfamily, including different subtypes of nAChRs, 5-HT_3A receptors (5-HT_3ARs), glycine receptors (GlyRs), and $GABA_A$ receptors ($GABA_A$Rs). α7nAChR is also homologous to GluCl, and the prokaryotic pLGICs ELIC and GLIC, whose crystal structures have been determined in the absence and presence of ligands (18–28). A wealth of data from decades of biochemical characterization and more recent structural characterization of pLGICs provide a broad understanding of the events relating to agonist binding and channel activation (28–35). Agonist binding to orthosteric sites in the ECD leads to conformational transitions that propagate through the ECD-TMD interface to the TMD and open the channel gate. Upon prolonged exposure to agonist, the channel desensitizes and is no longer sensitive to agonist binding until it returns to the resting state. Among pLGICs, α7nAChR demonstrates particularly rapid desensitization. PAMs such as ivermectin, PNU-120596, and TQS can significantly slow down the desensitization of α7nAChR (10, 11, 36, 37). Several studies have demonstrated involvement of the ECD-TMD interface in desensitization (38–41), but the role of the ECD-TMD interface in allosteric modulation through the TMD is less known.

* This work was supported, in whole or in part, by National Institutes of Health Grants R01GM66358 and R01GM56257 (to P. T.) and R37GM049202 (to Y. X.).
[1] To whom correspondence should be addressed: 2049 Biomedical Science Tower 3, 3501 Fifth Ave., University of Pittsburgh, Pittsburgh, PA 15260. Tel.: 412-383-9798; E-mail: tangp@upmc.edu.
[2] The abbreviations used are: α7nAChR, α7 nicotinic acetylcholine receptor; EA, ELIC-α7nAChR; ECD, extracellular domain; PAM, positive allosteric modulator; PDB, Protein Data Bank; pLGIC, pentameric ligand-gated ion channel; TMD, transmembrane domain.

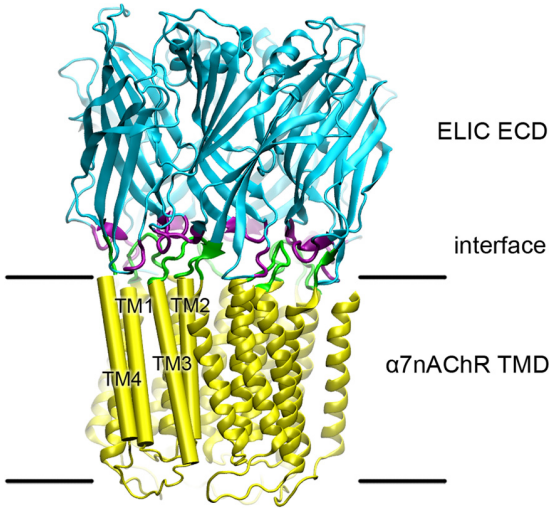

FIGURE 1. **Homology model of ELIC-α7nAChR highlighting the interface between domains.** The EA chimera was modeled to the ECD of ELIC (PDB ID code 3RQW) and the TMD of the α7nAChR (PDB ID code 2MAW). *Colors* depict the ELIC ECD (*cyan*) and the α7nAChR TMD (*yellow*). Residues predicted to comprise the ECD-TMD interface are colored *purple* in the ECD and *green* in the TMD. For clarity, the TMD helices of one subunit are labeled and depicted as *cylinders*.

Chimeras joining the ECD from one pLGIC with the TMD from another provide valuable opportunities to understand how the interplay among different domains/regions underlies pLGIC function. Previous studies of GLIC-α1GlyR (42), α7nAChR-α1GlyR (43), α4β2nAChR-5HT$_3$R (44), and α7nAChR-5HT$_3$R (45) found that functional chimeras could be obtained by splicing the ECD prior to the first transmembrane helix of the TMD, although kinetic parameters could be improved by optimization of the ECD-TMD interface. In contrast, it has proven difficult to express a functional chimera of an α7nAChR TMD (13). A 5HT$_3$R-α7nAChR chimera expressed a small current in only a few oocytes, which was sufficient to show that potentiation by the PAM PNU-120596 could be conferred by the α7nAChR TMD when activated by a suboptimal agonist (13). However, given the high homology between loop 7 and the TM2-3 linker of α7nAChR and 5HT$_3$R (approximately 78% similarity), it is unclear what role the ECD-TMD interface might have played in the observed potentiation.

In this study, we constructed multiple chimeras combining the TMD of human α7nAChR and the ECD of the prokaryotic homolog ELIC (Fig. 1). ELIC is a cation channel activated by a group of primary amines, including cysteamine (46). In contrast to α7nAChR, ELIC is inhibited by the general anesthetic propofol but unaffected by PAMs like ivermectin (21, 47). We show here that ELIC is also unaffected by the α7nAChR-specific PAMs PNU-120596 and TQS. We examined the effect of the ECD-TMD interface on allosteric modulation through the TMD by engineering two classes of ELIC-α7nAChR (EA) chimeras: EA$_{ELIC}$, with an ECD-TMD interface resembling ELIC, and EA$_{\alpha 7}$, with an α7nAChR ECD-TMD interface. Both classes of EA chimeras resulted in functional channels with similar activation and desensitization kinetics. However, only EA$_{\alpha 7}$ retained sensitivity to the PAMs ivermectin, PNU, and TQS as well as the ability to be activated by 4BP-TQS. Thus, allosteric modulation through the TMD requires a specific ECD-TMD interface similar to that of α7nAChR, a more stringent requirement than that needed to activate the channel by agonists.

EXPERIMENTAL PROCEDURES

Construction of EA Chimeras—EA chimeras were constructed by fusing the ECD of ELIC ending after pre-TM1 (ELIC-S201) with the beginning of the human α7nAChR TMD (α7-Y210) using overlapping PCR (48). The resulting construct was subcloned into a *Xenopus* expression vector, pOTV (49) for expression of RNA. Mutations to match the sequence of interface elements between ELIC and α7nAChR were introduced using QuikChange Lightning Site-directed Mutagenesis kits (Agilent). All constructs were confirmed by sequencing in full.

Electrophysiological Recordings in Xenopus Oocytes—Channel function was measured by two-electrode voltage clamp experiments (50) using *Xenopus laevis* oocytes injected with RNA encoding the indicated constructs as described previously (20). Capped complementary RNA was synthesized with the mMessage mMachine T7 kit (Ambion), purified with the RNeasy kit (Qiagen) and injected (25–50 ng) into *X. laevis* oocytes (stages 5–6). Oocytes were maintained at 18 °C in modified Barth's solution containing 88 mM NaCl, 1 mM KCl, 2.4 mM $NaHCO_3$, 15 mM HEPES, 0.3 mM $Ca(NO_3)_2$, 0.41 mM $CaCl_2$, 0.82 mM $MgSO_4$, 10 μg/ml sodium penicillin, 10 μg/ml streptomycin sulfate, and 100 μg/ml gentamycin sulfate, pH 6.7. After 1–3 days expression, oocytes were clamped to a holding potential of −60 mV with an OC-725C Amplifier (Warner Instruments) in a 20-μl oocyte recording chamber (Automate Scientific). Currents were elicited using cysteamine as an agonist. The recording solutions contained 130 mM NaCl, 0.1 mM $CaCl_2$, 10 mM HEPES, pH 7.0, with the indicated concentrations of cysteamine and other modulators. Data were collected and processed using Clampex 10 software (Molecular Devices). Nonlinear regressions were performed using Prism software (GraphPad).

Modeling of Chimeras—Homology models for EA chimeras were generated using Modeler 9v8 (51, 52) based on the crystal structure of ELIC (Protein Data Bank (PDB) ID code 3RQW) and the NMR structure of the α7nAChR TMD (PDB ID code 2MAW). Five independent models were generated, and the model with the lowest discrete optimized potential energy was selected for presentation.

RESULTS

Engineering Functional EA Chimeras—Multiple EA chimeras were constructed to assess the requirements for efficient coupling at the ECD-TMD interface. The function of each chimera was tested in *Xenopus* oocytes by two-electrode voltage clamp electrophysiology. The data for agonist response are summarized in Table 1.

The original ECD-TMD interfaces for ELIC and α7nAChR are not compatible. A chimera (EA$_{ELIC}^{1}$) simply connecting the ELIC ECD with the α7nAChR TMD at the beginning of TM1 did not show any response to the ELIC agonist cysteamine when the chimera was expressed in *Xenopus* oocytes (Table 1). This was unexpected. Chimeras between most members of the pLGIC family were found to have at least some degree of function when joined in this manner (13, 42–45), with the exception of the AChBP-5HT$_3$A chimeras (53). To rule out interference

TABLE 1
EA chimeras

The sequences for each ECD-TMD interface element modified in this study and their EC_{50}s for cysteamine are indicated. Residues from α7nAChR are indicated in bold. Residues conserved between the two sequences are italicized. Residues within the TM2-3 linker shown in the structures of ELIC (PDB ID code 3RQW) and α7nAChR (PDB ID code 2MAW) are underlined. A dash indicates no current detected.

Construct	Loop 2	Loop 7	Loop 9	Pre-TM1	TM2-3 linker	C terminus	Cysteamine EC_{50} (mM)
ELIC	NTLE	F***R***L	EEID***EW***W	NPS	SNILPRLPYTT	RGITL	0.4
α7nAChR	**DEKN**	**V*R*W**	**IPNG*EW*D**	**RTL**	**AEIMPATSDSVPLIAQY**	**SAPNFVEAVSKDFA**	—
EA_{ELIC}^{1}	NTLE	F***R***L	EEID***EW***W	NPS	**AEIMPATSDSVPLIAQY**	**SAPNFVEAVSKDFA**	—
EA_{ELIC}^{2}	NTLE	F***R***L	EEID***EW***W	NPS	**AEIMPATSDSVPLIAQY**	RGITL	—
EA_{ELIC}^{3}	NTLE	F***R***L	EEID***EW***W	NPS	**AEIM**PRLPY**SVPLIAQY**	RGITL	—
EA_{ELIC}^{4}	NTLE	F***R***L	EEID***EW***W	NPS	SNILPRLPYT**VPLIAQY**	RGITL	—
EA_{ELIC}^{5}	NTLE	F***R***L	EEID***EW***W	NPS	**AEI**LPRLPYTT----------	RGITL	0.4
EA_{ELIC}	NTLE	F***R***L	EEID***EW***W	NPS	A**P**RLPYTT**DSVPLIAQY**	RGITL	1.0
$EA_{\alpha7}^{1}$	NTLE	**V*R*W**	**IPNG*EW*D**	**RTL**	**AEIMPATSDSVPLIAQY**	RGITL	2.2
$EA_{\alpha7}^{2}$	**DEKN**	**V*R*W**	EEID***EW***W	**RTL**	**AEIMPATSDSVPLIAQY**	RGITL	2.6
$EA_{\alpha7}^{3}$	NTLE	**V*R*W**	EEID***EW***W	**RTL**	**AEIMPATSDSVPLIAQY**	RGITL	—
$EA_{\alpha7}^{4}$	**DEKN**	F***R***L	**IPNG*EW*D**	**RTL**	**AEIMPATSDSVPLIAQY**	RGITL	—
$EA_{\alpha7}$	**DEKN**	**V*R*W**	**IPNG*EW*D**	**RTL**	**AEIMPATSDSVPLIAQY**	RGITL	1.3

by the extended C terminus of α7nAChR, we replaced the last 18 residues of EA_{ELIC}^{1} with the last 4 residues of ELIC. This construct EA_{ELIC}^{2} also failed to exhibit current in response to cysteamine (Table 1).

The sequence, length, and position of the TM2-3 linker vary among the known pLGIC structures. The TM2-3 linker comprises 8 residues beginning at 22′ in ELIC (PDB ID code 3RQU) (20) and 10 residues beginning at 22′ in the NMR structure for the TMD of α7nAChR (PDB ID code 2MAW) (54). The TM2-3 linker in the cryo-EM structure of *Torpedo* nAChR has only 7 residues in the flexible loop beginning at 29′. If one counts the TM2-3 linker of *Torpedo* nAChR starting from 22′, it has a total of 14 residues (PDB ID code 2BG9) (55). A recent disulfide trapping experiment with the α subunit of mouse muscle nAChR showed a shift in register between TM2 and TM3, which could not be reconciled with 2BG9 (56), but was consistent with the α7 NMR structure (54).

To improve coupling of the α7nAChR TM2-3 linker to the ELIC ECD without disrupting TMD interactions, we substituted varied lengths of the TM2-3 linker in α7nAChR with their counterparts in ELIC. Substitution of only 4 residues in the middle of the TM2-3 linker (EA_{ELIC}^{3}) or more extensive substitution from 19′ to 28′ (EA_{ELIC}^{4}) was not functional (Table 1).

A functional EA chimera (EA_{ELIC}^{5}) was obtained by replacing all 14 residues from 22′ to 35′ of the TM2-3 region with the 8-residue ELIC TM2-3 linker. A functional EA chimera (EA_{ELIC}) was also obtained by substituting the α7nAChR TM2-3 linker from 20′ to 26′ with the ELIC TM2-3 linker from 23′ to 29′. Both EA_{ELIC}^{5} and EA_{ELIC} responded efficiently to the ELIC agonist cysteamine, with EC_{50} values of 0.4 and 1.0 mM, respectively (Table 1 and Fig. 2), comparable with that for ELIC (20, 46). The efficient activation obtained with both EA_{ELIC}^{5} and EA_{ELIC} compared with EA_{ELIC}^{3} and EA_{ELIC}^{4} suggests that it is not the length of the TM2-3 linker, but its position at the ECD-TMD interface that is critical for efficient coupling.

To engineer a chimera with a more native α7nAChR ECD-TMD interface, we kept the α7nAChR TM2-3 linker intact but mutated the ELIC ECD to match the sequence of α7nAChR at loops 2, 7, 9, and the pre-TM1 region. This construct, $EA_{\alpha7}$, is functional with an EC_{50} of 1.3 mM for cysteamine (Table 1 and Fig. 2). EA chimeras with mismatches at loop 2 ($EA_{\alpha7}^{1}$) or loop 9 ($EA_{\alpha7}^{2}$) still expressed as functional channels, but with a rightward shift in EC_{50} for cysteamine, suggesting a lower coupling efficiency (Table 1 and Fig. 2*c*). Mismatches at both loop 2 and loop 9 ($EA_{\alpha7}^{3}$), or at loop 7 alone ($EA_{\alpha7}^{4}$), resulted in chimeras that did not exhibit current in response to cysteamine (Table 1). Taken together, these results suggest that an ensemble of coupling among loop 2, loop 7, loop 9, the pre-TM1 region and the TM2-3 linker is essential for obtaining functional channels. Similar modifications were also needed for the functional AChBP-$5HT_3$ chimera (53).

ELIC (46) and α7nAChR (1) exhibit desensitization with sustained application of agonist, but α7nAChR (0.18 ± 0.05 min, $n = 3$) desensitizes an order of magnitude faster than ELIC (2.4 ± 0.2 min, $n = 3$) (Fig. 3). Measuring ensemble currents in *Xenopus* oocytes, both $EA_{\alpha7}$ and EA_{ELIC} exhibited initial desensitization (1.7 ± 0.2 and 1.6 ± 0.2 min, respectively, $n = 3$) comparable with ELIC, but then plateaued at 55 ± 11% and 74 ± 16% of the maximal current, respectively (Fig. 3).

$EA_{\alpha7}$ Shows Pharmacology Similar to α7nAChR, but EA_{ELIC} Does Not—ELIC and α7nAChR have different pharmacological profiles for allosteric modulators. Consistent with previous results (13–16, 57), ivermectin and two α7-specific PAMs, PNU-120596 and TQS, potentiated α7nAChR, but the intravenous general anesthetic propofol had no effects on α7nAChR (Fig. 4). In contrast, ELIC could be inhibited by propofol (21, 47)

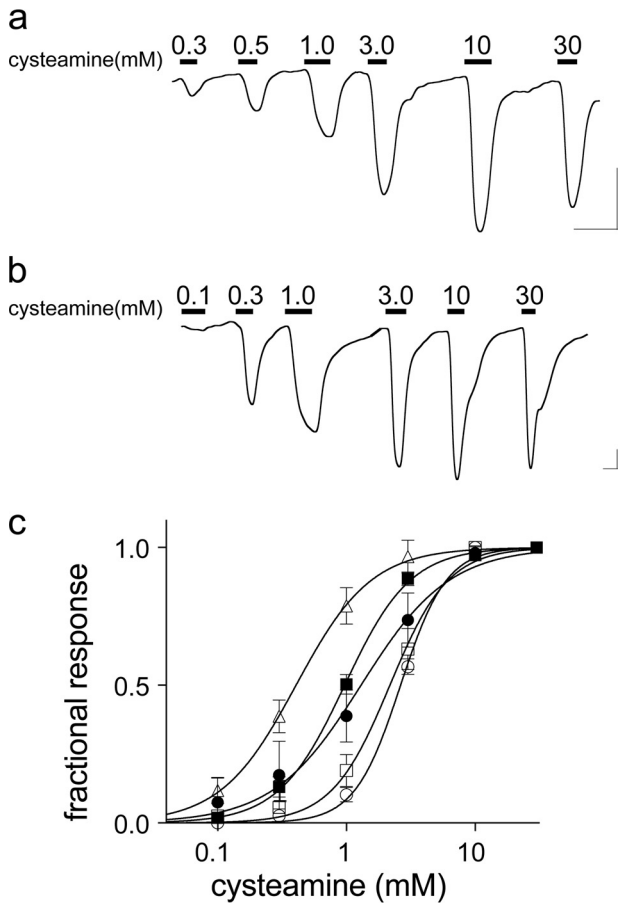

FIGURE 2. **Activation of EA chimeras by cysteamine.** *a* and *b*, representative current traces for EA_{ELIC} (*a*) and $EA_{\alpha7}$ (*b*). *Bars* over the *trace* indicate the length of application and cysteamine concentrations. *Horizontal* and *vertical scale bars* indicate 1 min and 0.1 μA current, respectively. *c*, cysteamine response curves for the functional EA chimeras. Current is expressed as a fraction of maximal current, $n \geq 5$ oocytes. *Error bars* indicate S.D. Data are fit to Hill equations with the following parameters: ■, EA_{ELIC}, $EC_{50} = 1.0 \pm 0.02$ mM; ●, $EA_{\alpha7}$, $EC_{50} = 1.3 \pm 0.1$ mM; △, $EA_{ELIC}{}^{5}$, $EC_{50} = 0.4 \pm 0.02$ mM; □, $EA_{\alpha7}{}^{1}$, $EC_{50} = 2.2 \pm 0.1$ mM; ○, $EA_{\alpha7}{}^{2}$, $EC_{50} = 2.6 \pm 0.1$ mM. The corresponding Hill coefficients are 1.7 ± 0.1, 1.3 ± 0.1, 1.5 ± 0.1, 1.9 ± 0.1, and 2.4 ± 0.2, respectively.

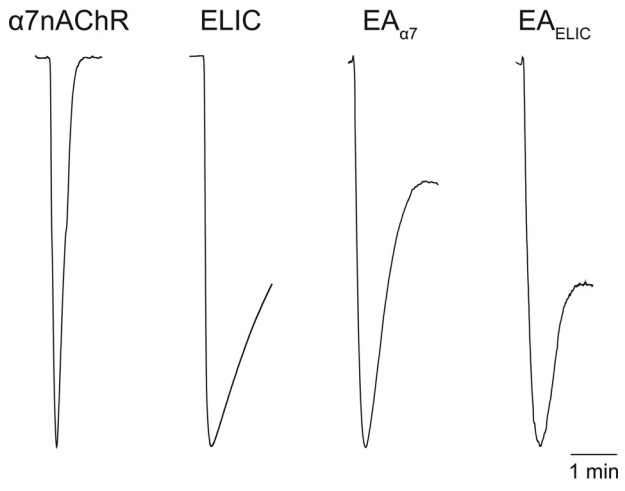

FIGURE 3. **EA chimeras desensitize much more slowly than α7nAChR.** Representative current traces show a 1.5-min agonist application to *Xenopus* oocytes injected with the indicated constructs. Acetylcholine at 100 μM was applied to α7nAChR; 30 mM cysteamine was applied to ELIC and EA chimeras. Rate constants for the initial rate of desensitization were calculated ($n = 3$): α7nAChR $= 0.18 \pm 0.05$; ELIC $= 2.4 \pm 0.2$; $EA_{ELIC} = 1.6 \pm 0.2$; and $EA_{\alpha7} = 1.7 \pm 0.2$ min.

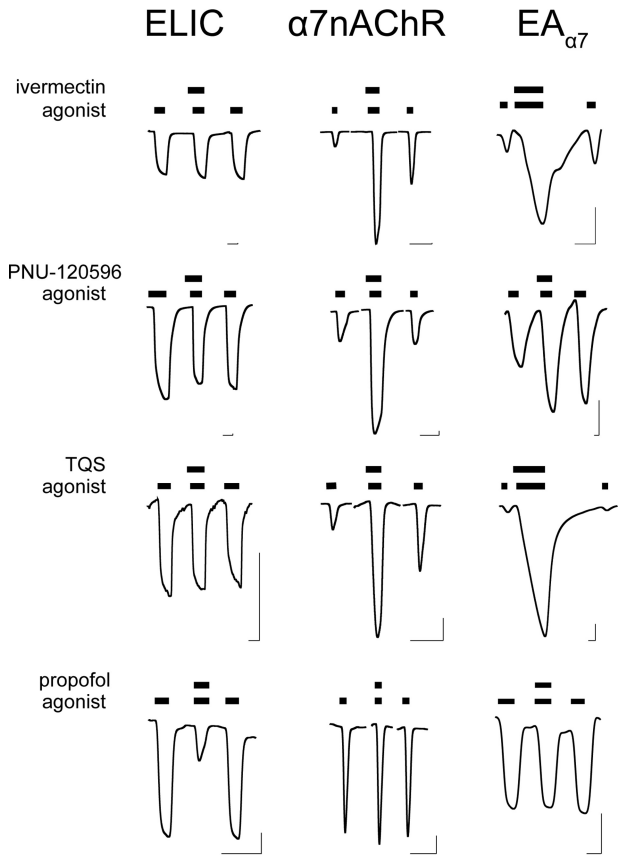

FIGURE 4. **$EA_{\alpha7}$ resembles α7nAChR pharmacology.** Representative traces of ELIC, α7nAChR, and $EA_{\alpha7}$ show responses to the indicated allosteric modulators. Ivermectin (30 μM), TQS (100 μM), and propofol (100 μM) were applied with agonist cysteamine (ELIC, $EA_{\alpha7}$) or acetylcholine (α7nAChR) at the EC_{20} for each construct; PNU-120596 (30 μM) was applied with agonist at the EC_{70} for each construct. *Bars* over the *traces* indicate the length of application. *Horizontal* and *vertical scale bars* indicate 1 min and 0.1 μA current, respectively.

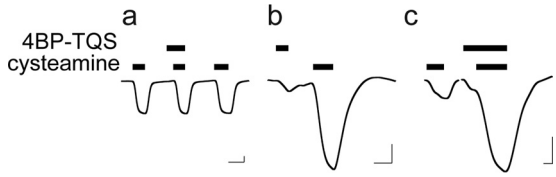

FIGURE 5. **$EA_{\alpha7}$ is activated and potentiated by 4BP-TQS.** Representative traces of ELIC and $EA_{\alpha7}$ show responses to cysteamine and 4BP-TQS. *a*, ELIC is insensitive to 4BP-TQS, but $EA_{\alpha7}$ is activated (*b*) and potentiated (*c*) by 4BP-TQS (100 μM). Cysteamine concentrations are at the EC_{20} for each construct. *Horizontal* and *vertical scale bars* indicate 1 min and 0.1 μA current, respectively.

but was insensitive to ivermectin, PNU-120596, or TQS (Fig. 4). The differences between ELIC and α7 pharmacology present the opportunity to evaluate the role of the TMD and ECD-TMD interface in allosteric modulation. To this end, we compared the functional responses of α7nAChR, ELIC, and $EA_{\alpha7}$ to the selected allosteric modulators (Fig. 4).

$EA_{\alpha7}$ responded to these modulators similarly to α7nAChR, but distinctly different from ELIC. Resembling α7nAChR, $EA_{\alpha7}$ was potentiated by ivermectin, PNU-120596, and TQS, and insensitive to propofol (Fig. 4). 4BP-TQS, an allosteric agonist and PAM for α7nAChR (15), could also directly activate $EA_{\alpha7}$ and potentiate its channel response to agonist (Fig. 5).

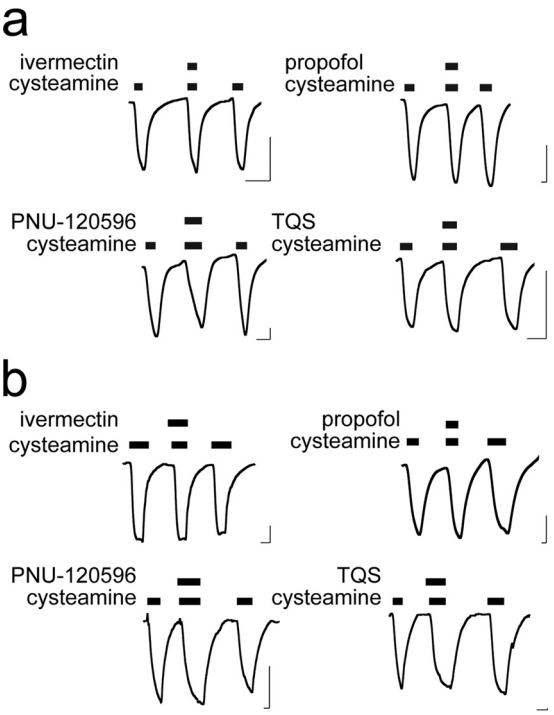

FIGURE 6. **EA_{ELIC} is insensitive to allosteric modulators acting through the TMD.** Representative traces of EA_{ELIC} (*a*) and EA_{ELIC}^{5} (*b*) show responses to the indicated allosteric modulators. Ivermectin (30 μM), TQS (100 μM), and propofol (100 μM) were applied with cysteamine at the EC_{20}; PNU-120596 (30 μM) was applied with cysteamine at the EC_{70}. *Bars* over the *traces* indicate length of application. *Horizontal* and *vertical scale bars* indicate 1 min and 0.1 μA current, respectively.

These results show that $EA_{\alpha 7}$ qualitatively reproduces the pharmacological properties of α7nAChR for these modulators.

In contrast to $EA_{\alpha 7}$, EA_{ELIC}^{5} and EA_{ELIC} were insensitive to ivermectin, TQS, or PNU-120596 (Fig. 6). They were also insensitive to propofol. The lack of sensitivity to propofol for the EA chimeras can be explained by the loss of the binding site within the ELIC TMD. However, EA_{ELIC}^{5}, EA_{ELIC}, and $EA_{\alpha 7}$ all have the α7nAChR TMD, which contains the binding sites for the tested PAMs. These chimeras differ only in the ECD-TMD interface, suggesting a functional role of the ECD-TMD interface in allosteric potentiation through the TMD.

DISCUSSION

Unlike other Cys-loop receptor chimeras (42–45), the engineering of functional chimeras between ELIC and α7nAChR requires more extensive optimization of an ensemble of interactions at the ECD-TMD interface. It does not matter how the optimization is achieved: chimeras with either an ELIC interface (EA_{ELIC}^{5}, EA_{ELIC}) or an α7nAChR interface ($EA_{\alpha 7}$) show similar agonist response and desensitization characteristics. They desensitize much slower than native α7nAChR. PAM modulation through the TMD only occurs with the α7nAChR ECD-TMD interface, suggesting that PAM modulation through the TMD requires a more specific ECD-TMD interface than agonist activation.

One of the primary effects noted for PAMs like PNU-120596 and TQS is a marked decrease in the α7nAChR desensitization rate (10, 11, 36, 37). Our study shows that $EA_{\alpha 7}$ does not reproduce the fast desensitization characteristic of α7nAChR, yet can still be modulated by these PAMs, suggesting that fast desensitization may not be required for potentiation by PNU-120596 or TQS. Because $EA_{\alpha 7}$ and EA_{ELIC} show similar desensitization rates, desensitization cannot explain their distinct responses to the tested PAMs.

What may have contributed to the different responses of $EA_{\alpha 7}$ and EA_{ELIC} to PAMs? The PAMs tested here bind to the TMD (13–15, 58). The differences between $EA_{\alpha 7}$ and EA_{ELIC}/EA_{ELIC}^{5} are localized only to the ECD-TMD interface. One may suspect that lack of modulation in EA_{ELIC}^{5} results from interference with PAMs binding to a structurally distorted TMD due to a shortened TM2-3 linker. However, such a possibility is dismissed by EA_{ELIC}, which has a full-length TM2-3 linker that is unlikely to distort the TMD.

Because no high resolution structural data are available, the precise binding sites for ivermectin, PNU-120596, or TQS in α7nAChR are unknown. In the *Caenorhabditis elegans* GluCl crystal structure, ivermectin contacts both the TM2-3 linker and the residues toward the middle of the TMD (18). Mutational analysis on α7nAChR also suggests that ivermectin interacts with residues near the TM2-3 linker and residues near the middle of the TMD (16, 59). If direct contacts to specific residues in the TM2-3 linker are critical for ivermectin modulation, the ELIC TM2-3 linker may not provide proper contacts in EA_{ELIC} and EA_{ELIC}^{5}, thereby preventing ivermectin modulation.

In the case of PNU-120596 and TQS, they are much smaller than ivermectin and cannot simultaneously contact residues at both the ECD-TMD interface and near the middle of the TMD. If they directly contact the ECD-TMD interface, the role of the ECD-TMD interface in PAM modulation will be the same as discussed above for ivermectin. However, previous mutation studies suggest an intrasubunit binding site near the middle of the TMD for PNU-120596 and TQS (13–15, 58). In this case, the binding site is remote from the ECD-TMD interface. How can the interface still be important for modulation? It is possible that the PAM binding to the proposed site near the middle of TMD allosterically induces changes to the ECD-TMD interface that are required for potentiation. These changes can be accommodated by the ECD-TMD interface in α7nAChR, but not in ELIC. This hypothesis is supported by a substituted cysteine accessibility study (60), which demonstrates that PNU-120596 binding can independently induce conformational changes to the ECD and ECD-TMD interface. The conformational changes induced by PNU-120596 are similar but not identical to those induced by the agonist acetylcholine (60).

Structural characterization of the precise binding sites for these PAMs is essential for understanding the mechanism of PAM modulation. Future high resolution structural studies of the EA chimeras in the absence and presence of modulators will provide insights into binding of PAMs to the TMD and the role of the ECD-TMD interface in allosteric modulation. Because of the prokaryotic origin of its ECD, the EA chimeras are good candidates for production in quantities suitable for high resolution structural studies (19, 20).

Acknowledgment—We thank Prof. Thomas R. Kleyman's laboratory for providing X. laevis oocytes for electrophysiology experiments.

REFERENCES

1. Couturier, S., Bertrand, D., Matter, J. M., Hernandez, M. C., Bertrand, S., Millar, N., Valera, S., Barkas, T., and Ballivet, M. (1990) A neuronal nicotinic acetylcholine receptor subunit (α7) is developmentally regulated and forms a homo-oligomeric channel blocked by α-BTX. *Neuron* **5,** 847–856
2. Wessler, I., and Kirkpatrick, C. J. (2008) Acetylcholine beyond neurons: the nonneuronal cholinergic system in humans. *Br. J. Pharmacol.* **154,** 1558–1571
3. Alsharari, S. D., Freitas, K., and Damaj, M. I. (2013) Functional role of α7 nicotinic receptor in chronic neuropathic and inflammatory pain: studies in transgenic mice. *Biochem. Pharmacol.* **86,** 1201–1207
4. de Jonge, W. J., and Ulloa, L. (2007) The α7 nicotinic acetylcholine receptor as a pharmacological target for inflammation. *Br. J. Pharmacol.* **151,** 915–929
5. Wang, H., Yu, M., Ochani, M., Amella, C. A., Tanovic, M., Susarla, S., Li, J. H., Wang, H., Yang, H., Ulloa, L., Al-Abed, Y., Czura, C. J., and Tracey, K. J. (2003) Nicotinic acetylcholine receptor α7 subunit is an essential regulator of inflammation. *Nature* **421,** 384–388
6. Egleton, R. D., Brown, K. C., and Dasgupta, P. (2008) Nicotinic acetylcholine receptors in cancer: multiple roles in proliferation and inhibition of apoptosis. *Trends Pharmacol. Sci.* **29,** 151–158
7. Poorthuis, R. B., and Mansvelder, H. D. (2013) Nicotinic acetylcholine receptors controlling attention: behavior, circuits and sensitivity to disruption by nicotine. *Biochem. Pharmacol.* **86,** 1089–1098
8. Pandya, A. A., and Yakel, J. L. (2013) Effects of neuronal nicotinic acetylcholine receptor allosteric modulators in animal behavior studies. *Biochem. Pharmacol.* **86,** 1054–1062
9. Smucny, J., and Tregellas, J. (2013) Nicotinic modulation of intrinsic brain networks in schizophrenia. *Biochem. Pharmacol.* **86,** 1163–1172
10. Hurst, R. S., Hajós, M., Raggenbass, M., Wall, T. M., Higdon, N. R., Lawson, J. A., Rutherford-Root, K. L., Berkenpas, M. B., Hoffmann, W. E., Piotrowski, D. W., Groppi, V. E., Allaman, G., Ogier, R., Bertrand, S., Bertrand, D., and Arneric, S. P. (2005) A novel positive allosteric modulator of the α7 neuronal nicotinic acetylcholine receptor: *in vitro* and *in vivo* characterization. *J. Neurosci.* **25,** 4396–4405
11. Grønlien, J. H., Håkerud, M., Ween, H., Thorin-Hagene, K., Briggs, C. A., Gopalakrishnan, M., and Malysz, J. (2007) Distinct profiles of α7 nAChR positive allosteric modulation revealed by structurally diverse chemotypes. *Mol. Pharmacol.* **72,** 715–724
12. Grønlien, J. H., Ween, H., Thorin-Hagene, K., Cassar, S., Li, J., Briggs, C. A., Gopalakrishnan, M., and Malysz, J. (2010) Importance of M2-M3 loop in governing properties of genistein at the α7 nicotinic acetylcholine receptor inferred from α7/5-HT3A chimera. *Eur. J. Pharmacol.* **647,** 37–47
13. Bertrand, D., Bertrand, S., Cassar, S., Gubbins, E., Li, J., and Gopalakrishnan, M. (2008) Positive allosteric modulation of the α7 nicotinic acetylcholine receptor: ligand interactions with distinct binding sites and evidence for a prominent role of the M2-M3 segment. *Mol. Pharmacol.* **74,** 1407–1416
14. Young, G. T., Zwart, R., Walker, A. S., Sher, E., and Millar, N. S. (2008) Potentiation of α7 nicotinic acetylcholine receptors via an allosteric transmembrane site. *Proc. Natl. Acad. Sci. U.S.A.* **105,** 14686–14691
15. Gill, J. K., Savolainen, M., Young, G. T., Zwart, R., Sher, E., and Millar, N. S. (2011) Agonist activation of α7 nicotinic acetylcholine receptors via an allosteric transmembrane site. *Proc. Natl. Acad. Sci. U.S.A.* **108,** 5867–5872
16. Collins, T., and Millar, N. S. (2010) Nicotinic acetylcholine receptor transmembrane mutations convert ivermectin from a positive to a negative allosteric modulator. *Mol. Pharmacol.* **78,** 198–204
17. Collins, T., Young, G. T., and Millar, N. S. (2011) Competitive binding at a nicotinic receptor transmembrane site of two α7-selective positive allosteric modulators with differing effects on agonist-evoked desensitization. *Neuropharmacology* **61,** 1306–1313
18. Hibbs, R. E., and Gouaux, E. (2011) Principles of activation and permeation in an anion-selective Cys-loop receptor. *Nature* **474,** 54–60
19. Hilf, R. J., and Dutzler, R. (2008) X-ray structure of a prokaryotic pentameric ligand-gated ion channel. *Nature* **452,** 375–379
20. Pan, J., Chen, Q., Willenbring, D., Yoshida, K., Tillman, T., Kashlan, O. B., Cohen, A., Kong, X. P., Xu, Y., and Tang, P. (2012) Structure of the pentameric ligand-gated ion channel ELIC cocrystallized with its competitive antagonist acetylcholine. *Nat. Commun.* **3,** 714
21. Spurny, R., Ramerstorfer, J., Price, K., Brams, M., Ernst, M., Nury, H., Verheij, M., Legrand, P., Bertrand, D., Bertrand, S., Dougherty, D. A., de Esch, I. J., Corringer, P. J., Sieghart, W., Lummis, S. C., and Ulens, C. (2012) Pentameric ligand-gated ion channel ELIC is activated by GABA and modulated by benzodiazepines. *Proc. Natl. Acad. Sci. U.S.A.* **109,** E3028–E3034
22. Bocquet, N., Nury, H., Baaden, M., Le Poupon, C., Changeux, J. P., Delarue, M., and Corringer, P. J. (2009) X-ray structure of a pentameric ligand-gated ion channel in an apparently open conformation. *Nature* **457,** 111–114
23. Hilf, R. J., and Dutzler, R. (2009) Structure of a potentially open state of a proton-activated pentameric ligand-gated ion channel. *Nature* **457,** 115–118
24. Nury, H., Van Renterghem, C., Weng, Y., Tran, A., Baaden, M., Dufresne, V., Changeux, J. P., Sonner, J. M., Delarue, M., and Corringer, P. J. (2011) X-ray structures of general anaesthetics bound to a pentameric ligand-gated ion channel. *Nature* **469,** 428–431
25. Spurny, R., Billen, B., Howard, R. J., Brams, M., Debaveye, S., Price, K. L., Weston, D. A., Strelkov, S. V., Tytgat, J., Bertrand, S., Bertrand, D., Lummis, S. C., and Ulens, C. (2013) Multisite binding of a general anesthetic to the prokaryotic pentameric *Erwinia chrysanthemi* ligand-gated ion channel (ELIC). *J. Biol. Chem.* **288,** 8355–8364
26. Gonzalez-Gutierrez, G., Lukk, T., Agarwal, V., Papke, D., Nair, S. K., and Grosman, C. (2012) Mutations that stabilize the open state of the *Erwinia chrysanthemi* ligand-gated ion channel fail to change the conformation of the pore domain in crystals. *Proc. Natl. Acad. Sci. U.S.A.* **109,** 6331–6336
27. Gonzalez-Gutierrez, G., Cuello, L. G., Nair, S. K., and Grosman, C. (2013) Gating of the proton-gated ion channel from *Gloeobacter violaceus* at pH 4 as revealed by x-ray crystallography. *Proc. Natl. Acad. Sci. U.S.A.* **110,** 18716–18721
28. Sauguet, L., Shahsavar, A., Poitevin, F., Huon, C., Menny, A., Nemecz, À., Haouz, A., Changeux, J. P., Corringer, P. J., and Delarue, M. (2014) Crystal structures of a pentameric ligand-gated ion channel provide a mechanism for activation. *Proc. Natl. Acad. Sci. U.S.A.* **111,** 966–971
29. Dacosta, C. J., and Baenziger, J. E. (2013) Gating of pentameric ligand-gated ion channels: structural insights and ambiguities. *Structure* **21,** 1271–1283
30. Bouzat, C. (2012) New insights into the structural bases of activation of Cys-loop receptors. *J. Physiol.* **106,** 23–33
31. Corringer, P. J., Poitevin, F., Prevost, M. S., Sauguet, L., Delarue, M., and Changeux, J. P. (2012) Structure and pharmacology of pentameric receptor channels: from bacteria to brain. *Structure* **20,** 941–956
32. Smart, T. G., and Paoletti, P. (2012) Synaptic neurotransmitter-gated receptors. *Cold Spring Harb. Perspect. Biol.* **4,** a009662
33. Auerbach, A. (2010) The gating isomerization of neuromuscular acetylcholine receptors. *J. Physiol.* **588,** 573–586
34. Sine, S. M., and Engel, A. G. (2006) Recent advances in Cys-loop receptor structure and function. *Nature* **440,** 448–455
35. Chang, Y., Huang, Y., and Whiteaker, P. (2010) Mechanism of allosteric modulation of the Cys-loop receptors. *Pharmaceuticals* **3,** 2592–2609
36. Krause, R. M., Buisson, B., Bertrand, S., Corringer, P. J., Galzi, J. L., Changeux, J. P., and Bertrand, D. (1998) Ivermectin: a positive allosteric effector of the α7 neuronal nicotinic acetylcholine receptor. *Mol. Pharmacol.* **53,** 283–294
37. Bertrand, D., and Gopalakrishnan, M. (2007) Allosteric modulation of nicotinic acetylcholine receptors. *Biochem. Pharmacol.* **74,** 1155–1163
38. Zhang, J., Xue, F., Whiteaker, P., Li, C., Wu, W., Shen, B., Huang, Y., Lukas, R. J., and Chang, Y. (2011) Desensitization of α7 nicotinic receptor is governed by coupling strength relative to gate tightness. *J. Biol. Chem.* **286,** 25331–25340
39. Bouzat, C., Bartos, M., Corradi, J., and Sine, S. M. (2008) The interface between extracellular and transmembrane domains of homomeric Cys-loop receptors governs open-channel lifetime and rate of desensitization. *J. Neurosci.* **28,** 7808–7819

40. Wang, Q., and Lynch, J. W. (2011) Activation and desensitization induce distinct conformational changes at the extracellular-transmembrane domain interface of the glycine receptor. *J. Biol. Chem.* **286,** 38814–38824
41. Keramidas, A., and Lynch, J. W. (2013) An outline of desensitization in pentameric ligand-gated ion channel receptors. *Cell. Mol. Life Sci.* **70,** 1241–1253
42. Duret, G., Van Renterghem, C., Weng, Y., Prevost, M., Moraga-Cid, G., Huon, C., Sonner, J. M., and Corringer, P. J. (2011) Functional prokaryotic-eukaryotic chimera from the pentameric ligand-gated ion channel family. *Proc. Natl. Acad. Sci. U.S.A.* **108,** 12143–12148
43. Grutter, T., de Carvalho, L. P., Dufresne, V., Taly, A., Edelstein, S. J., and Changeux, J. P. (2005) Molecular tuning of fast gating in pentameric ligand-gated ion channels. *Proc. Natl. Acad. Sci. U.S.A.* **102,** 18207–18212
44. Cooper, S. T., Harkness, P. C., Baker, E. R., and Millar, N. S. (1999) Up-regulation of cell-surface $\alpha4\beta2$ neuronal nicotinic receptors by lower temperature and expression of chimeric subunits. *J. Biol. Chem.* **274,** 27145–27152
45. Eiselé, J. L., Bertrand, S., Galzi, J. L., Devillers-Thiéry, A., Changeux, J. P., and Bertrand, D. (1993) Chimaeric nicotinic-serotonergic receptor combines distinct ligand binding and channel specificities. *Nature* **366,** 479–483
46. Zimmermann, I., and Dutzler, R. (2011) Ligand activation of the prokaryotic pentameric ligand-gated ion channel ELIC. *PLoS Biol.* **9,** e1001101
47. Thompson, A. J., Alqazzaz, M., Ulens, C., and Lummis, S. C. (2012) The pharmacological profile of ELIC, a prokaryotic GABA-gated receptor. *Neuropharmacology* **63,** 761–767
48. Higuchi, R., Krummel, B., and Saiki, R. K. (1988) A general method of *in vitro* preparation and specific mutagenesis of DNA fragments: study of protein and DNA interactions. *Nucleic Acids Res.* **16,** 7351–7367
49. Arriza, J. L., Fairman, W. A., Wadiche, J. I., Murdoch, G. H., Kavanaugh, M. P., and Amara, S. G. (1994) Functional comparisons of three glutamate transporter subtypes cloned from human motor cortex. *J. Neurosci.* **14,** 5559–5569
50. Dascal, N. (2001) in *Current Protocols in Neuroscience* (Crawley, J. N., McKay, R. A., and Rogawski, M. A., eds) Chapter 6, Unit 6.12, John Wiley and Sons, Hoboken, NJ
51. Eswar, N., Marti-Renom, M. A., Webb, B., Madhusudhan M. S., Eramian, D., Shen, M., Pieper, U., Sali, A. (2006) *Current Protocols in Bioinformatics*, Supplement 15, 5.6.1–5.6.30, John Wiley and Sons, Hoboken, NJ
52. Fiser, A., Do, R. K., and Sali, A. (2000) Modeling of loops in protein structures. *Protein Sci.* **9,** 1753–1773
53. Bouzat, C., Gumilar, F., Spitzmaul, G., Wang, H. L., Rayes, D., Hansen, S. B., Taylor, P., and Sine, S. M. (2004) Coupling of agonist binding to channel gating in an ACh-binding protein linked to an ion channel. *Nature* **430,** 896–900
54. Bondarenko, V., Mowrey, D. D., Tillman, T. S., Seyoum, E., Xu, Y., and Tang, P. (2014) NMR structures of the human $\alpha7$ nAChR transmembrane domain and associated anesthetic binding sites. *Biochim. Biophys. Acta* **1838,** 1389–1395
55. Unwin, N. (2005) Refined structure of the nicotinic acetylcholine receptor at 4 Å resolution. *J. Mol. Biol.* **346,** 967–989
56. Mnatsakanyan, N., and Jansen, M. (2013) Experimental determination of the vertical alignment between the second and third transmembrane segments of muscle nicotinic acetylcholine receptors. *J. Neurochem.* **125,** 843–854
57. Flood, P., Ramirez-Latorre, J., and Role, L. (1997) $\alpha4\beta2$ neuronal nicotinic acetylcholine receptors in the central nervous system are inhibited by isoflurane and propofol, but $\alpha7$-type nicotinic acetylcholine receptors are unaffected. *Anesthesiology* **86,** 859–865
58. daCosta, C. J., Free, C. R., Corradi, J., Bouzat, C., and Sine, S. M. (2011) Single-channel and structural foundations of neuronal $\alpha7$ acetylcholine receptor potentiation. *J. Neurosci.* **31,** 13870–13879
59. Sattelle, D. B., Buckingham, S. D., Akamatsu, M., Matsuda, K., Pienaar, I., Jones, A. K., Sattelle, B. M., Almond, A., and Blundell, C. D. (2009) Comparative pharmacology and computational modelling yield insights into allosteric modulation of human $\alpha7$ nicotinic acetylcholine receptors. *Biochem. Pharmacol.* **78,** 836–843
60. Barron, S. C., McLaughlin, J. T., See, J. A., Richards, V. L., and Rosenberg, R. L. (2009) An allosteric modulator of $\alpha7$ nicotinic receptors, *N*-(5-chloro-2,4-dimethoxyphenyl)-*N*′-(5-methyl-3-isoxazolyl)-urea (PNU-120596), causes conformational changes in the extracellular ligand binding domain similar to those caused by acetylcholine. *Mol. Pharmacol.* **76,** 253–263